AIP Journal of Applied Physics

Removal of end-of-range defects in Ge + -pre-amorphized Si by carbon ion implantation

Peng-Shiu Chen, T. E. Hsieh, and Chih-Hsun Chu

Citation: Journal of Applied Physics **85**, 3114 (1999); doi: 10.1063/1.369694
View online: http://dx.doi.org/10.1063/1.369694
View Table of Contents: http://scitation.aip.org/content/aip/journal/jap/85/6?ver=pdfcov
Published by the AIP Publishing

Articles you may be interested in

Ultrashallow (10 nm) p + n junction formed by B 18 H 22 cluster ion implantation and excimer laser annealing
Appl. Phys. Lett. **89**, 243516 (2006); 10.1063/1.2405863

Influence of dislocations in strained Si relaxed SiGe layers on n + p -junctions in a metal-oxide-semiconductor field-effect transistor technology
Appl. Phys. Lett. **87**, 192112 (2005); 10.1063/1.2128490

Impact of dislocation densities on n + p and p + n junction GaAs diodes and solar cells on SiGe virtual substrates
J. Appl. Phys. **98**, 014502 (2005); 10.1063/1.1946194

Annealing of ultrashallow p + /n junction by 248 nm excimer laser and rapid thermal processing with different preamorphization depths
Appl. Phys. Lett. **76**, 3197 (2000); 10.1063/1.126627

Effect of implant temperature on transient enhanced diffusion of boron in regrown silicon after amorphization by Si + or Ge + implantation
J. Appl. Phys. **81**, 6051 (1997); 10.1063/1.364391

AIP Publishing Re-register for Table of Content Alerts

Create a profile. Sign up today!

[This article is copyrighted as indicated in the article. Reuse of AIP content is subject to the terms at: http://scitation.aip.org/termsconditions. Downloaded to] IP: 140.113.38.11 On: Thu, 01 May 2014 08:43:23

Removal of end-of-range defects in Ge^+-pre-amorphized Si by carbon ion implantation

Peng-Shiu Chen and T. E. Hsieh
Department of Materials Science and Engineering, National Chiao Tung University, Hsinchu, Taiwan, Republic of China

Chih-Hsun Chu
United Silicon Inc., Hsinchu Science-based Industrial Park, Hsinchu, Taiwan, Republic of China

(Received 28 September 1998; accepted for publication 17 December 1998)

Carbon ion implantation was employed to annihilate the end-of-range (EOR) defects in Ge^+-pre-amorphized Si. Experimental results showed that the efficiency of EOR defect removal depends on the Ge^+-pre-amorphization conditions, the location of projected range (R_p) of carbon implant and subsequent annealing conditions. The best defect removal occurred when R_p of carbon implantation was brought close to the amorphous/crystalline (a/c) interface generated by Ge^+-pre-amorphization. The higher the annealing temperature, the better the interstitial gettering efficiency of carbon atoms was observed. However, transmission electron microscopy investigation revealed the emergence of hairpin dislocations when dose and accelerating voltage of Ge^+ implantation were high. In specimens without carbon implantation, the hairpin dislocations could be readily removed by a 900 °C, 30 min anneal. For carbon-implanted specimens, the density of hairpin dislocations increased when R_p of carbon implantation was close to the (a/c) interface. The glide motion of hairpin dislocations was affected by Ge^+-pre-amorphization conditions and was inhibited by the SiC complexes formed in the vicinity of dislocations so that they became rather difficult to anneal out of the specimens. © *1999 American Institute of Physics.* [S0021-8979(99)06306-9]

I. INTRODUCTION

The formation of shallow p^+/n junctions is more difficult than that of p/n^+ junctions in ultralarge-scale integration (ULSI) device fabrication. Among all techniques, ion implantation is a popular method to form shallow p^+/n junctions with desired junction depth in Si. It is often achieved with pre-amorphization[1,2] of *n*-type Si by implanting the nondoping ion species such as Si^+ or Ge^+ followed by the implantation of p^+-type impurity. The purpose of pre-amorphization is to prevent the channeling of lightly weight p^+-dopant elements such as boron (B).

For the specimens subjected to ion implantation, subsequent annealing treatment is a must in order to activate the dopants and to annihilate the primary crystalline defects generated by ion bombardment. However, during the collapse of primary defects, the secondary defects, also called the end-of-range (EOR) dislocation loops,[3] emerge near the original amorphous/crystalline (a/c) interface. The EOR defects are known to deteriorate the electrical properties of shallow p^+/n junctions. Furthermore, the excess interstitials may also combine with dopant atoms to induce the transient enhanced diffusion (TED) during the thermal process.[4,5] The removal of EOR defects hence becomes an important issue for ion implantation applied to shallow p^+/n junction fabrication.

There are many articles reporting the elimination of EOR defects in ion-implanted Si. Ajmera *et al.*[6] found that the EOR defects in Si^+- and Ge^+-pre-amorphized Si could be removed by a 1050 °C, 10 s rapid thermal annealing (RTA) process. The same RTA treatment was utilized by Hong *et al.* to eliminate the implantation damages in their low-energy ion implanted Si.[7] It was also proposed that the formation of certain types of silicides on Si surface may serve as a source of point defects.[8] The vacancies generated may diffuse into the Si substrate to combine with the excess interstitials and annihilate the EOR defects. An application of this method was presented by Wen *et al.*, who found that the density of EOR dislocation loops near a/c interface was reduced when titanium (Ti) silicide was grown onto the Si wafer surface.[9] Gettering is another favorite method for EOR defects removal. It has been shown that carbon atoms are effective gettering centers to capture metallic impurities in Si.[10] Nishikawa *et al.* adopted this concept and performed the carbon ion implantation to eliminate the EOR dislocation loops.[11] As the annealing treatment proceeded, the excess carbon atoms migrated to the Si interstitials and formed SiC agglomerates. They acted as a sink of excess Si interstitials, which resulted in a reduction of EOR defects. Incorporation of carbon and Si atoms was also found to be able to suppress the TED of boron dopants.[12,13] However, Liefting *et al.* reported that carbon implantation became ineffective to eliminate the EOR dislocation loops when boron dose was beyond $5\times10^{14}/cm^2$.[14] In such a dose condition, the displacement profile of carbon implants did not completely overlap with that generated by boron implants. This decreased the communication between the carbon and the damage generated by boron so that the inefficiency of EOR loop elimination was observed.[14]

This work describes the removal of EOR defects by carbon implantation in Ge^+-pre-amorphized Si. The gettering

 © 1999 American Institute of Physics

[This article is copyrighted as indicated in the article. Reuse of AIP content is subject to the terms at: http://scitation.aip.org/termsconditions. Downloaded to] IP: 140.113.38.11 On: Thu, 01 May 2014 08:43:23

TABLE I. Ion implantation conditions.

Sample	Implantation conditions Type of ion/energy (keV)/dose (cm^{-2})	Depth of a/c interface (nm)
D	$Ge^+/30/5\times10^{14}$; $Ge^+/400/1\times10^{14}$;	43.4
D-1	$Ge^+/30/5\times10^{14}$; $Ge^+/400/1\times10^{14}$; $C^+/90/1\times10^{15}$	~43.3
D-2	$Ge^+/30/5\times10^{14}$; $Ge^+/400/1\times10^{14}$; $C^+/200/1\times10^{15}$	~43.3
D-3	$Ge^+/30/5\times10^{14}$; $Ge^+/400/1\times10^{14}$; $C^+/350/1\times10^{15}$	~43.3
H	$Ge^+/30/5\times10^{14}$; $Ge^+/400/5\times10^{14}$;	440
H-1	$Ge^+/30/5\times10^{14}$; $Ge^+/400/5\times10^{14}$; $C^+/90/1\times10^{15}$	~440
H-2	$Ge^+/30/5\times10^{14}$; $Ge^+/400/5\times10^{14}$; $C^+/200/1\times10^{15}$	~440
H-3	$Ge^+/30/5\times10^{14}$; $Ge^+/400/5\times10^{14}$; $C^+/350/1\times10^{15}$	~440

efficiency of annealing treatments was investigated. It was found that the efficiency of carbon gettering strongly depends on the relative distance between projected range (R_p) of carbon implantation and the location of EOR defects. Furthermore, the tendency to form hairpin dislocations increased when Ge^+ pre-amorphization failed to produce a sharp a/c interface in Si.[15] In order to reduce the strain field of defects, SiC complexes would migrate toward the hairpin dislocations.[16] This would inhibit the glide motions of dislocations and hence their removal during further annealing.

II. EXPERIMENT

The 3–5 Ω cm, *n*-type, single crystalline Cz–Si (100) wafers (oxygen concentration less than $10^{18}\,cm^{-3}$) were the substrates used for this study. After a standard RCA cleaning process, ion implantations of Ge^+ and C^+ were then carried out in accordance with the conditions listed in Table I. Specimens were annealed in a nitrogen furnace at temperatures ranging from 550 to 950 °C for various times. A titanium getter apparatus heated to 800 °C was used to reduce the oxygen content in nitrogen gas before it entered the furnace tube. The specimens subjected to various annealing treatments were then thinned properly for subsequent microstructure observation. Both planview and cross-sectional transmission electron microscopy (PTEM and XTEM) specimens were prepared and a Hitachi-600 electron microscope was used to record their microstructure. The density of EOR dislocation loops was calculated by randomly selecting a $3\times3\,cm^2$ area on the PTEM micrograph of 30 000 times magnification imaged at the diffraction condition of $\mathbf{g}=[220]$. The image was then transferred to a personal computer equipped with image analyzing software (Ultimage from Graftek) to count the number and to calculate the area enclosed by dislocation loops. For each sample, at least one TEM micrograph was taken for the purpose of defect density calculation. The atoms bounded by EOR dislocation loops were counted by multiplying the EOR dislocation density with the mean loop area and the area density of atoms in {111} plane which is about equal to $1.6\times10^{15}/cm^2$. Full-cascade Monte Carlo simulations of carbon ion implanted at 90, 200, and 350 keV were performed with Trim 91.14[17] using a value of 12 eV[18] for displacement energy and 2 eV for the binding energy. At least 10 000 ions were brought in to simulate the value of R_p for each condition of carbon implantation.

III. RESULTS AND DISCUSSION

A. Ge^+-implanted specimens

It is known that the microstructure in the vicinity of a/c interface plays an important role in the formation of hairpin dislocations when solid phase epitaxy of the pre-amorphization layer proceeds.[15] The stresses around the transition region between amorphous and crystalline structure in Si may induce some small misoriented crystallites embedded in the amorphous layer near the a/c interface. During annealing, these misoriented crystallites act as the nucleation sites of hairpin dislocations. At the end of solid phase epitaxy, the ''V-shaped'' dislocations form by extending two characteristic branches to the specimen surface. During further annealing treatment, the hairpin dislocation reduces its length by migrating toward the surface in order to decrease its line energy. Sands *et al.* showed that the activation energy of hairpin dislocation migration is in the range of 2–2.5 eV.[15]

For the specimen H, the implantation energy and dose amount produced a continuous amorphous layer with thickness approximately equal to 440 nm. However, its a/c interface appears to be relatively rough, as shown in Fig. 1(a). After a 900 °C, 10 s annealing, the hairpin dislocations were observed, as shown in Fig. 1(b). As the time of annealing treatment increased, the hairpin dislocation glided out on a cylindrical glide plane defined by its Burgers vector and the direction of dislocation line.[15] According to our TEM analysis, the hairpin dislocations had a 1/2⟨110⟩-type Burgers vector and the average line direction along ⟨131⟩. No hairpin dislocation was observed in specimen H annealed over 30 min as illustrated in Fig. 1(c).

For the specimen D, the dose amount in the high-energy part of Ge^+ implantation was less than that for specimen H. This produced a 43.4 nm thick amorphous layer in conjunction with a damaged layer of 300 nm thickness, as shown in Fig. 2(a). After being heat treated at 800 °C for 30 min, EOR defects buried at the depth of 330 ± 80 nm from the specimen surface were observed, as shown in Fig. 2(b). The EOR defects diminished significantly and their range of distribution shrunk to about 90 nm after a 900 °C, 30 min annealing, as shown in Fig. 2(c). In all subsequent anneals no hairpin dislocation was observed in specimen D.

B. Ge^+ and C^+ implanted specimens

Comparing Figs. 3(a)–3(c) with Fig. 2(c), it is evident that much more EOR defects appear in D-series specimens

[This article is copyrighted as indicated in the article. Reuse of AIP content is subject to the terms at: http://scitation.aip.org/termsconditions. Downloaded to] IP: 140.113.38.11 On: Thu, 01 May 2014 08:43:23

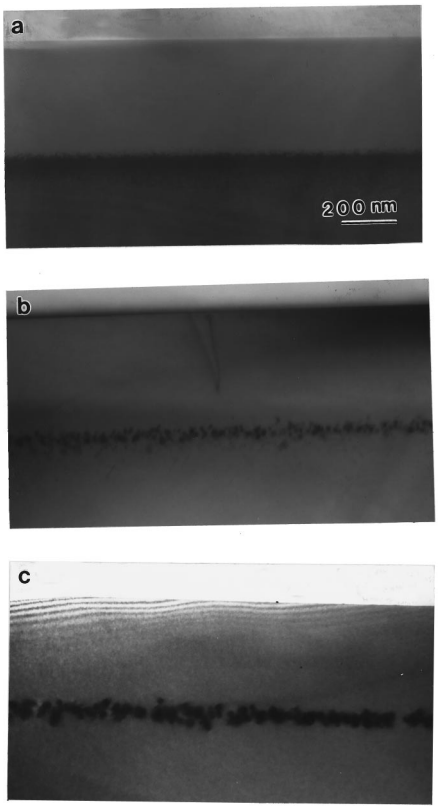

FIG. 1. Cross-sectional view of specimen H: (a) as implanted, (b) annealed at 900 °C for 10 s, (c) annealed at 900 °C for 30 min.

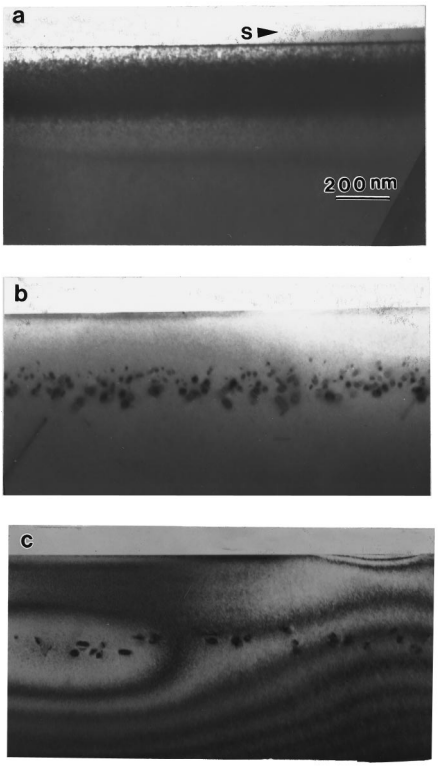

FIG. 2. Cross-sectional view of specimen D: (a) as implanted, (b) annealed at 800 °C for 30 min, (c) annealed at 900 °C for 30 min. (S: specimen surface).

implanted with carbon after a 900 °C, 30 min annealing. Figures 3(a)–3(c) also show that the distribution of EOR defects in D-series specimens with carbon implantation is much wider than that in the specimen without carbon implantation. Apparently none of the carbon implantation processes applied to D-series specimens were able to suppress the formation of EOR defects. Cacciato *et al.* reported the combination of excess carbon atoms with Si interstitials to form SiC complexes in Si matrix.[16] In D-series specimens, most of the implanted carbon atoms were probably captured by the widely spread Si interstitials in a damaged layer to form SiC complexes which, in turn, prohibit the elimination of EOR defects from the specimen.

The XTEM and PTEM micrographs of H-series specimens, subjected to 900 °C, 30 min annealing, were shown in Figs. 4(a)–4(c) and Figs. 5(a)–5(d), respectively. It is clear that the H-2 specimen contains the smallest amount of EOR defects after annealing. Our computer simulation results indicated the projected ranges of H-1, H-2, and H-3 were 246.4, 498.3, and 760.3 nm, respectively. Among these, the projected range of H-2 specimen would be the closest to the EOR defects located at the depth of about 400 nm from the specimen surface. Since it was the site where most of the excess Si interstitials locate, the H-2 specimen would have the highest amount of SiC complexes and hence the best annihilation efficiency of EOR loops. Our calculation showed that the concentration of interstitial atoms bounded by EOR loops would be $2.61\times10^{14}/\mathrm{cm}^2$, $1.08\times10^{14}/\mathrm{cm}^2$,

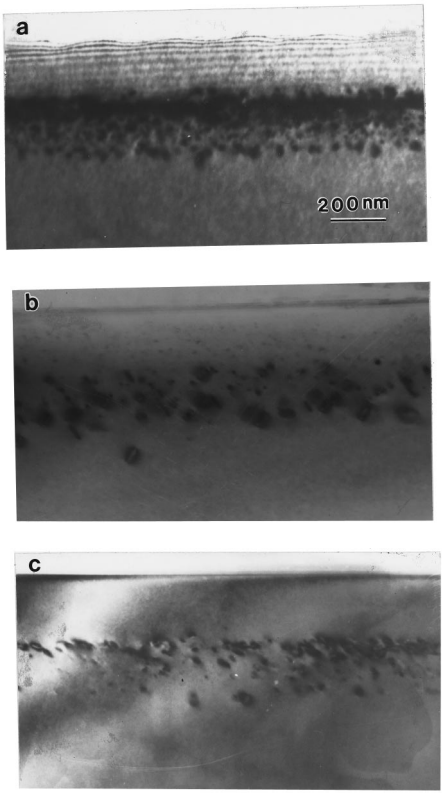

FIG. 3. Cross-sectional view of specimen (a) D-1, (b) D-2, (c) D-3 annealed at 900 °C for 30 min.

[This article is copyrighted as indicated in the article. Reuse of AIP content is subject to the terms at: http://scitation.aip.org/termsconditions. Downloaded to] IP: 140.113.38.11 On: Thu, 01 May 2014 08:43:23

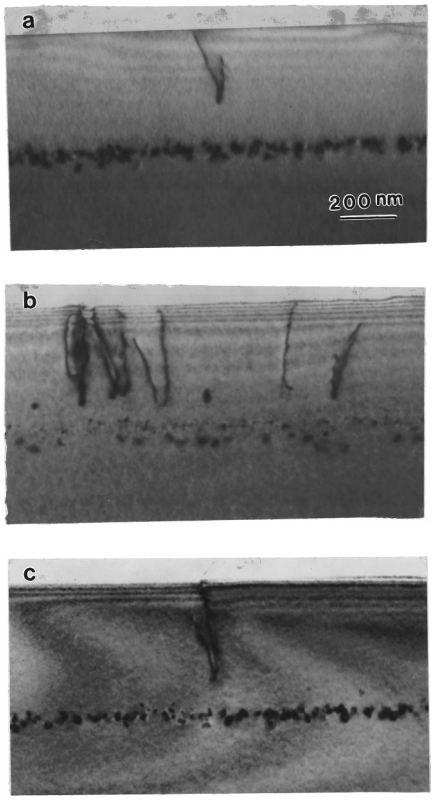

FIG. 4. Cross-sectional view of specimen (a) H-1, (b) H-2, (c) H-3 annealed at 900 °C for 30 min.

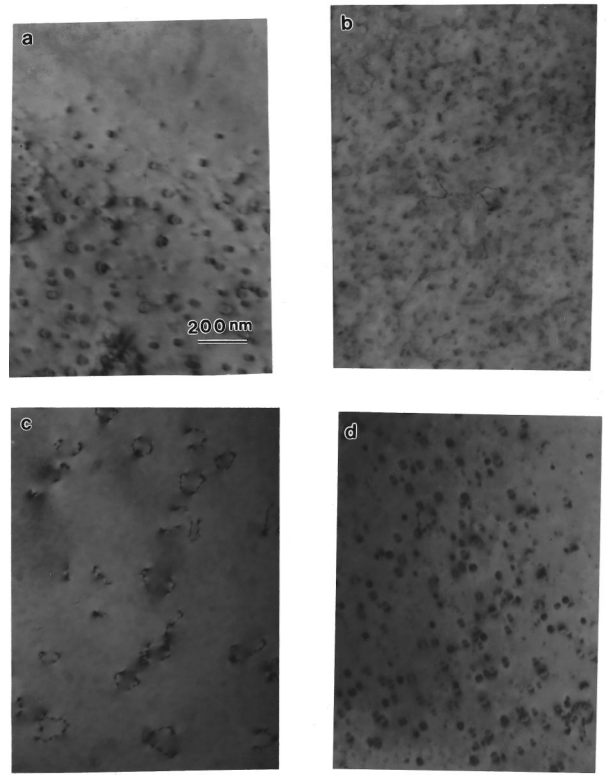

FIG. 5. Planview TEM micrograph of specimen (a) H, (b) H-1, (c) H-2, (d) H-3 annealed at 900 °C for 30 min.

$2.23\times10^{13}/\mathrm{cm}^2$, and $2.22\times10^{13}/\mathrm{cm}^2$ for H, H-1, H-2, and H-3 specimens annealed at 900 °C for 30 min. For the H-2 specimen, nearly 91% of interstitials were eliminated during the annealing treatment.

Though all the H-series specimens exhibited, a certain degree of carbon gettering effect for defect annihilation, hairpin dislocations also emerged in these specimens, as evidenced in Figs. 4(a)–4(c) and Figs. 5(a)–5(d). Transmission electron microscopy revealed that they were the dislocations with $1/2\langle 110\rangle$-type Burgers vectors, which is the same as those reported by Seidel *et al.*[19] Our calculation revealed that the density of hairpin dislocations in the H-2 specimen ($\sim7\times10^8/\mathrm{cm}^2$) was higher than that in the H-1 specimen ($\sim1\times10^8/\mathrm{cm}^2$) and in the H-3 specimen ($\sim2\times10^8/\mathrm{cm}^2$). We also observed that in the specimens without carbon implantation, the hairpin dislocations were able to glide swiftly and eventually moved out of the specimens by a 900 °C, 30 min annealing. As to the specimens implanted with carbon subjected to the same thermal process, migration of hairpin dislocations was rather obscure. This may be attributed to the solute drag effect of SiC complexes, which severely limits the mobility of dislocations.

The distribution of hairpin dislocations in H-series specimens annealed at 900 °C for long times was also investigated. Though some dislocations changed their line arrangement into an irregular shape, the hairpin dislocation density in H-2 specimens were virtually the same after a 2 h treatment [see Fig. 6(a)]. For H-3 specimens subjected to the same thermal treatment, some dislocations changed their sharp V-shaped tip into a smooth concave curve and a certain degree of glide out motion was observed [see Fig. 6(b)]. For an H-2 specimen annealed at 900 °C for 6 h, the hairpin dislocation persisted, as shown in Fig. 6(c). Since the retardation of dislocation motion would be less in H-3 specimens, a 900 °C, 6 h annealing hence was able to remove the hairpin dislocations in H-3 specimens, as shown in Fig. 6(d).

C. The effects of temperature

It was reported by Kang and Schroder that annealing temperature affects the gettering efficiency of impurities in Si.[20] Their study showed that, for instance, in Ar ion implanted Si the optimum gettering of gold (Au) impurity occurs at the temperature around 900 °C. Figures 7(a) and 7(b) are the PTEM images of H-2 specimens annealed at 700 and 800 °C for 30 min. Comparing the density of EOR defects in these specimens with that in 900 °C-annealed specimen [see Fig. 5(c)], it is obvious that the best EOR defect annihilation occurs in the specimen subjected to 900 °C annealing. Our TEM results also showed that the change of annealing temperature did not help very much to eliminate the hairpin dislocations in H-2 specimen. We raised the annealing temperature to 950 °C for 30 min and, as shown in Fig. 8, the hairpin dislocations were still observed in the H-2 specimen.

Figures 9(a) and 9(b) show the XTEM and PTEM micrographs of the H-3 specimen annealed at 550 °C for 30 min. It can be readily seen that the density of hairpin dislocations in this specimen is higher than that in the specimen annealed at 900 °C for 30 min [see Fig. 5(d)]. Since the solute drag effect occurred to a lesser extent in the H-3 specimen and the mobility of dislocations would be higher when

[This article is copyrighted as indicated in the article. Reuse of AIP content is subject to the terms at: http://scitation.aip.org/termsconditions. Downloaded to] IP: 140.113.38.11 On: Thu, 01 May 2014 08:43:23

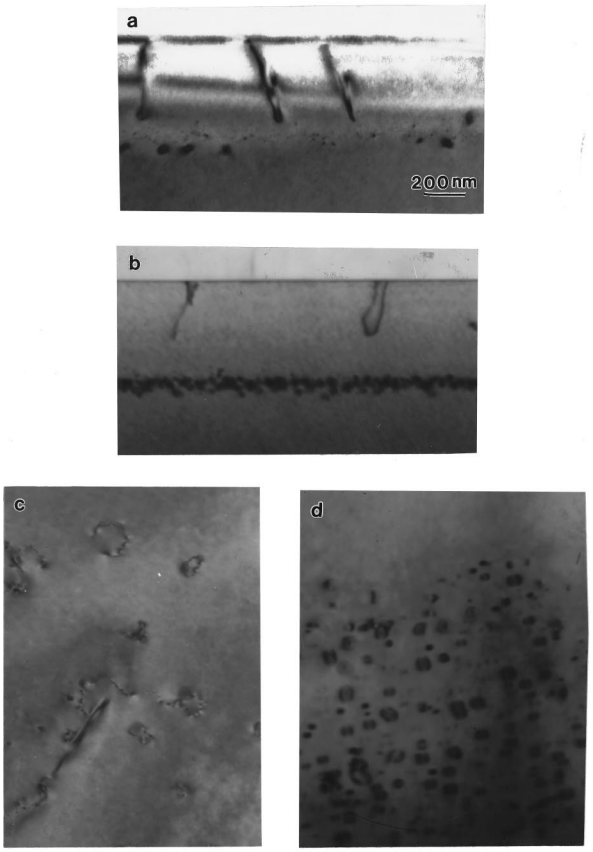

FIG. 6. Cross-sectional view of specimen (a) H-2 annealed at 900 °C for 2 h, (b) H-3 annealed at 900 °C for 2 h, and planview TEM micrograph of specimen (c) H-2 annealed at 900 °C for 6 h. (d) H-3 annealed at 900 °C for 6 h.

annealing temperature was raised, some of the hairpin dislocations were able to glide out of the specimen annealed at 900 °C for 30 min.

Myers *et al.* carried out a very low temperature anneal (VLTA) process to sharpen the a/c interface in

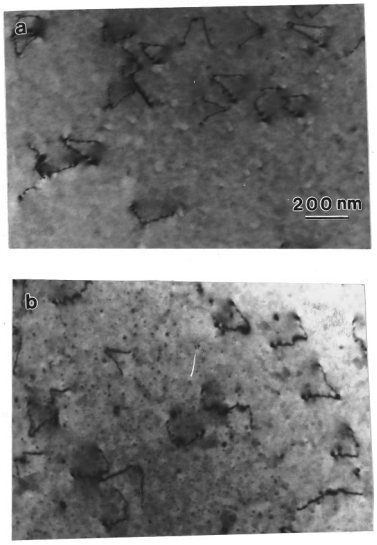

FIG. 7. Planview TEM micrograph of specimen H-2 annealed at (a) 700 °C, (b) 800 °C for 30 min.

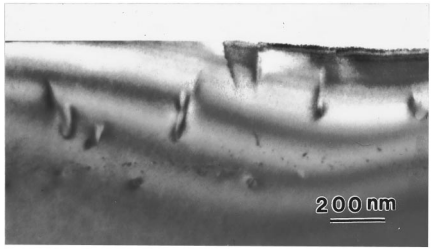

FIG. 8. Cross-sectional view of specimen H-2 annealed at 950 °C for 30 min.

Ge^+-implanted Si.[21] The purpose of this process was to shorten the transition region between amorphous and crystalline structure in Si so as to suppress the generation of hairpin dislocations. In our work the H-2 specimen was treated by a two-step thermal process consisting of a 400 °C, 1 h annealing followed by a 900 °C, 30 min annealing. However, no significant reduction of hairpin dislocations was observed, as revealed by TEM investigation shown in Figs. 10(a) and 10(b). We believe this resulted from the pinning effect of SiC complexes and that the thermal agitation provided by our annealing treatment is insufficient to activate the migration of SiC-decorated dislocations.

IV. CONCLUSIONS

Our study demonstrates that carbon implantation is an effective method to remove the EOR defects in ion implanted Si. The small carbon atoms were able to combine with excess Si interstitials to form a SiC complex gettering center. The closer the projected range of carbon implantation to the location of EOR defects, the better the gettering efficiency for defect removal. However, the effect of defect annihilation was only obvious when sharp a/c interface was formed by Ge^+-pre-amorphization. Otherwise, the implanted

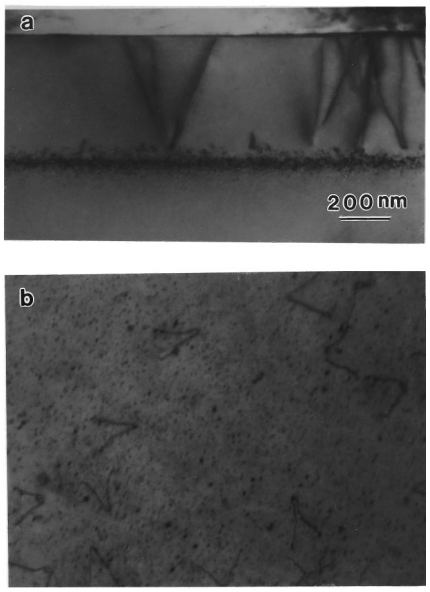

FIG. 9. (a) Cross-sectional view of specimen H-3 annealed at 550 °C for 6 h and (b) corresponding planview micrograph of (a).

[This article is copyrighted as indicated in the article. Reuse of AIP content is subject to the terms at: http://scitation.aip.org/termsconditions. Downloaded to] IP: 140.113.38.11 On: Thu, 01 May 2014 08:43:23

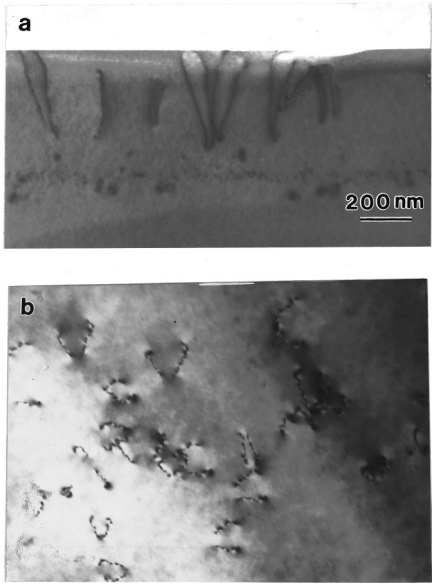

FIG. 10. (a) Cross-sectional view of specimen H-2 annealed at 400 °C for 1 h followed by 900 °C annealing for 30 min and (b) corresponding planview micrograph of (a).

carbon atoms were captured by the widely spread Si interstitials and their defect annihilation ability was hence limited.

Investigation of hairpin dislocations in H-series specimens showed that the density of dislocations increased with the increase of dose and accelerating voltage of Ge^+ implantation conditions. For specimens without carbon implantation, the hairpin dislocations were able to glide out of the specimen after a 900 °C, 30 min annealing. However, in the specimens subjected to carbon implantation the same thermal treatment could not remove the dislocations effectively. This is attributed to the solute drag effect resulting from the formation of SiC complexes in the vicinity of dislocations. Our study also shows that the gettering effect of carbon implantation depends on the temperature of subsequent annealing. The best defect annihilation was observed in the specimens subjected to 900 °C annealing. The two-step annealing did not improve the hairpin dislocation removal in the specimen with carbon implantation. This is due to the insufficient thermal energy to activate the migration of dislocations pinned by SiC complexes.

[1] M. C. Ozturk and J. J. Wortman, Appl. Phys. Lett. **52**, 281 (1988).
[2] A. J. Walker, P. H. Woeriee, H. G. Pomp, and N. E. B. Cowern, J. Appl. Phys. **73**, 4048 (1993).
[3] K. S. Jones, S. Prussin, and E. R. Weber, Appl. Phys. A: Solids Surf. **45**, 1 (1988).
[4] J. Thorton, K. C. Paus, R. P. Webb, I. H. Wilson, and G. R. Booker, J. Appl. Phys. **21**, 334 (1988).
[5] T. O. Sedgwick, A. E. Michel, V. R. Deline, S. A. Cohen, and J. B. Lasky, J. Appl. Phys. **63**, 1452 (1988).
[6] A. C. Ajmera, G. A. Rozgonyi, and R. B. Fair, Appl. Phys. Lett. **52**, 813 (1988).
[7] S. N. Hong, G. A. Rozgonzi, J. J. Wortman, and M. C. Ozturk, IEEE Trans. Electron Devices **38**, 476 (1991).
[8] S. M. Hu, Appl. Phys. Lett. **51**, 308 (1987).
[9] D. S. Wen, P. L. Smith, C. M. Osburn, and G. A. Rozgonzi, Appl. Phys. Lett. **51**, 1182 (1987).
[10] H. Wong, N. W. Cheung, K. M. Yu, P. K. Chu, and J. Liu, Mater. Res. Soc. Symp. Proc. **147**, 97 (1989).
[11] S. Nishikawa, A. Yanaka, and T. Yamaji, Appl. Phys. Lett. **60**, 2270 (1992).
[12] S. Isomae, T. Ishiba, T. Ando, and M. Tamura, J. Appl. Phys. **74**, 3815 (1993).
[13] P. A. Stolk, D. J. Eaglesham, H. J. Grossmann, and J. M. Poate, Appl. Phys. Lett. **66**, 1370 (1995).
[14] J. R. Liefting, J. S. Custer, and F. W. Saris, Mater. Res. Soc. Symp. Proc. **235**, 179 (1992).
[15] T. Sands, J. Washburn, R. Gronsky, W. Maszara, D. Sadana, and G. A. Rozgonyi, in *13th International Conference on Defect Semiconductors*, edited by L. C. Kimerling and J. M. Parsev, Jr. (The Metallurgical Society of AIME, New York, 1984), p. 531.
[16] A. Cacciato, J. G. E. Klappe, N. E. B. Cowern, W. Vandervost, L. P. Biró, J. S. Cluster, and F. W. Saris, J. Appl. Phys. **79**, 2314 (1996).
[17] J. P. Biersack and L. G. Haggmark, Nucl. Instrum. Methods **174**, 257 (1980).
[18] J. Narayan, D. Fathy, O. S. Oen, and O. W. Holland, J. Vac. Sci. Technol. A **2**, 1303 (1984).
[19] T. E. Seidel, D. M. Maher, and R. V. Knoell, in Ref. 15, p. 523.
[20] J. S. Kang and D. K. Schroder, J. Appl. Phys. **65**, 2974 (1989).
[21] E. Myers, G. A. Rozgonyi, D. K. Sadana, W. Maszara, J. J. Wortman, and J. Narayan, Mater. Res. Soc. Symp. Proc. **52**, 107 (1986).

[This article is copyrighted as indicated in the article. Reuse of AIP content is subject to the terms at: http://scitation.aip.org/termsconditions. Downloaded to] IP: 140.113.38.11 On: Thu, 01 May 2014 08:43:23